

# Identification of the potential molecular targets for human intervertebral disc degeneration based on bioinformatic methods

JIAXUAN HE<sup>1</sup>, RONGLIANG XUE<sup>1</sup>, SIYUAN LI<sup>1</sup>, JIANRUI LV<sup>1</sup>, YONG ZHANG<sup>1</sup>,  
LIYING FAN<sup>2</sup>, YUNPENG TENG<sup>1</sup> and HAIDONG WEI<sup>1</sup>

Departments of <sup>1</sup>Anesthesiology and <sup>2</sup>Orthopedics, The Second Affiliated Hospital of Xi'an,  
Jiaotong University, Xi'an, Shaanxi 710004, P.R. China

Received June 16, 2015; Accepted September 30, 2015

DOI: 10.3892/ijmm.2015.2389

**Abstract.** The present study aimed to explore potential molecular targets and gain further insights into the mechanism of intervertebral disc degeneration (IDD) progression. Microarray datasets of GSE19943, GSE15227 and GSE34095 were downloaded from the Gene Expression Omnibus database. Differentially expressed genes (DEGs) in 3 IDD specimens compared with 3 controls in GSE34095, DEGs in 7 grade III and 3 grade IV samples compared with 5 grade II samples in GSE19943, and differentially expressed miRNAs in 3 degenerated samples compared with 3 controls in GSE15227 were screened. Grade III- and IV-specific networks were constructed and grade-specific genes were extracted. The network features were analyzed, followed by Gene Ontology (GO) enrichment analysis and pathway enrichment analysis of grade-specific genes and DEGs identified in GSE34095. Furthermore, miRNA-pathway interactions were analyzed using Fisher's exact test. Tumor protein p53 (*TP53*) was a hub gene in the grade III-specific network and ubiquitin C (*UBC*) was identified to be a hub gene in the grade IV-specific network. Six significant features were identified by grade-specific network topology analysis. Grade-specific genes and DEGs were involved in different GO terms and pathways. Differentially expressed miRNAs were identified to participate in 35 pathways, among which 6 pathways were significantly enriched by DEGs, including apoptosis. The present study identified that key genes (*TP53* and *UBC*) and miR-129-5p may participate in the mechanism of IDD progression. Thus, they may be potential therapeutic targets for IDD.

## Introduction

Intervertebral disc degeneration (IDD) is characterized by damage of the disc structure, progressive loss of water content and proteoglycan in the extracellular matrix (ECM) (1). IDD is considered a predominant source of spine-related diseases and chronic lower back pain, which causes a major economic and social burden affecting millions of people worldwide (2). Current treatment options for IDD, including discectomy (3), intradiscal electrothermal therapy (4) and arthroplasty (5), only address the clinical symptoms of IDD and remain limited with unpredictable outcomes (6). Therefore, understanding the pathophysiology and molecular mechanism underlying IDD appears to be imperative for diagnosis and developing novel therapeutic approaches.

The intervertebral disc consists of three morphologically distinct regions, which are the nucleus pulposus (NP), annulus fibrosis and cartilaginous endplates (7). The central NP is a gelatinous matrix that is composed of large aggregating proteoglycans and a loose network of collagen. The peripheral annulus fibrosis encases the nucleus pulposus and is rich in type I collagen. The cartilaginous endplates contain the peripheral vasculature, which can nourish the disc (1). The main morphological manifestations of IDD are vertebral instability, disc herniation and spinal stenosis (8). Significant changes in morphology, structure and composition are accompanied by specific changes in the disc with aging and degeneration, including alteration of the elastic modulus and swelling pressure of the nucleus pulposus (9). Recently, histological grading schemes for assessing human IDD have been developed (10,11). A 5-level grading system for lumbar disc degeneration, proposed by Pfirrmann *et al* (11), was developed according to T2-weighted magnetic resonance images. Additionally, the Thompson scoring system scores disc degeneration over the spectrum from healthier discs (grades I and II) to advanced degeneration (grade V, the most advanced stage of degeneration) (10). However, there is a lack of studies on the associations of the grades of disc degeneration.

IDD is a complex multi-factorial process (12). Several factors, such as biological, mechanical and genetic factors, are widely considered as significant contributors to the disc degenerative process (1). For example, Bachmeier *et al* (13) identified that matrix metalloproteinase-3 (MMP-3), which was essential for matrix degeneration, had an essential role in lumbar disc

---

*Correspondence to:* Dr Rongliang Xue, Department of Anesthesiology, The Second Affiliated Hospital of Xi'an, Jiaotong University, 157 West 5th Road, Xi'an, Shaanxi 710004, P.R. China  
E-mail: rongliangx@163.com

**Key words:** intervertebral disc degeneration, differentially expressed genes, differentially expressed miRNAs, grade-specific genes, pathway enrichment analysis

herniation and degeneration. Additionally, Takahashi *et al* (14) revealed that the polymorphism 5A allele, which often occurs in the promoter region of the gene that regulates MMP-3 expression, was a possible risk factor for accelerated IDD in the elderly. In addition, Pratsinis *et al* (15) reported that platelet-derived growth factor, insulin-like growth factor-I and basic fibroblast growth factor could stimulate the proliferation of intervertebral disc cells via the activation of the extracellular-signal regulated kinase and Akt signaling pathways. By contrast, microRNAs (miRNAs) that can regulate RNA degradation or repression of translation have been identified as key regulators in numerous biological processes (16). Recently, Yu *et al* (17) demonstrated that miR-10b could promote nucleus pulposus cell proliferation by targeting homeobox D10 through the ras homolog family member C-Akt pathway in IDD. However, the molecular mechanism of IDD is not fully understood and further investigations are required.

Recently, Chen *et al* (18) reported that mitogen-activated protein (MAP) kinase kinase 6 (MAP2K6) and Ras homologous-related BTB domain containing 2 may have significant roles in the progression of grade III and IV disc degeneration, respectively. Additionally, Tang *et al* (8) demonstrated that differentially expressed genes (DEGs) identified in degenerative disc tissue samples were mainly associated with transforming growth factor- $\beta$  and the ECM. Furthermore, Wang *et al* (19) reported that deregulated miR-155 could promote Fas-mediated apoptosis in human IDD by targeting Fas-associated death domain-containing protein (FADD) and caspase-3. In the present study, 3 microarray datasets were integrated and microarray analysis was used to identify the DEGs, grade-specific genes and differentially expressed miRNAs in the IDD samples compared with their corresponding controls. In addition, comprehensive bioinformatics was used to analyze the significant functions and pathways, and to analyze the miRNA-target gene-pathway interaction associations. The study aimed to identify the significant genes and miRNA alternations in the progression of IDD and gain more insights into the molecular mechanisms of disc degeneration. Understanding these mechanisms can aid in exploring an appropriate molecular target and developing new therapeutic methods for IDD.

## Materials and methods

**Microarray data.** Microarray datasets of GSE19943 (19), GSE15227 (20) and GSE34095 (21) were downloaded from the National Center of Biotechnology Information (NCBI), Gene Expression Omnibus (GEO) database (<http://www.ncbi.nlm.nih.gov/geo/>). The miRNA expression profile GSE19943 included 3 degenerative NP samples that were collected from patients with IDD and 3 NP controls derived from patients with scoliosis, which was based on the platform GPL9946 Exiqon human miRCURY LNA™ microRNA Array V11.0. The GSE15227 dataset included 5 grade II, 7 grade III, and 3 grade IV discs from patients with herniated discs and IDD that were scored using the Thompson scoring system, which was based on the platform GPL1352 [U133\_X3P] Affymetrix Human X3P array. The gene expression profile GSE34095 included 3 degenerative NP samples that were harvested from elderly patients with IDD and 3 non-degenerative samples derived from younger patients with adolescent idiopathic

scoliosis as controls, which was based on the platform GPL96 [HG-U133A] Affymetrix Human Genome U133A array.

**DEGs and differentially expressed miRNAs screening.** The t-test in the limma package (22) was used to identify DEGs in degenerative samples compared with controls in GSE34095, DEGs in 7 grade III and 3 grade IV samples compared with 5 grade II samples in GSE15227, and to identify differentially expressed miRNAs in 3 degenerated samples compared with controls in GSE19943. The false discovery rate (FDR) was applied to perform multiple testing corrections using the Benjamini and Hochberg method (23). The threshold for the DEGs and the differentially expressed miRNAs were set as FDR <0.05.

**miRNA-target gene and KEGG pathway data collection.** Human miRNAs and their associated targets were downloaded from 3 high-quality online miRNA reference databases, which store manual collections of experimentally supported miRNA targets, miRecords (24), miRTarBase (25) and TarBase 6.0 (26). In addition, all pathways and associated genes were downloaded from the Kyoto Encyclopedia of Genes and Genomes (KEGG) database (27).

**Grade-specific network construction.** DEGs identified in grade III and IV samples were imported into Cytoscape software (28) to create protein-protein interaction (PPI) network visualizations, respectively. The source of the interaction network database was the Search Tool of the Retrieval of Interacting Genes 9.0 database, which is a comprehensive database containing functional links between proteins that are experimentally derived, as well as links predicted by text mining and comparative genomics (29). The threshold was set as confidence score, 0.4. Furthermore, the specific genes that were only enriched in one of the grade-specific networks and the common genes of the 2 grade-specific networks were extracted. The parameters describing the network topology were calculated using the Cytoscape plugin Network Analyzer (30). Logistic regression analysis (31) was conducted by SPSS 19.0 (IBM, Corp., Armonk, NY, USA) to select the most noteworthy network features.

**Cluster analysis.** To test the availability of these 2 grade-specific networks to reveal different stages of IDD progression, clustering analysis was performed on all genes in the networks and the top 20% nodes that had a higher degree in the network using Cytoscape plugin Network Analyzer (30), respectively. The results are represented by heat-maps.

**GO and pathway enrichment analysis of DEGs and the specific genes.** GO and KEGG enrichment analysis were performed for the specific genes using the Database for Annotation, Visualization and Integrated Discovery (DAVID) online tool (32). The threshold was set as P<0.05.

Furthermore, KEGG enrichment analyses were also performed for DEGs that were identified based on GSE34095 using DAVID. The threshold was set as P<0.05.

**Measurement of miRNA-pathway interactions.** With the identified differentially expressed miRNAs, as well as their target genes and the genes enriched in the KEGG pathways,

Fisher's exact test (33) was used to assess the corresponding significance of the miRNA pathway.

Fisher's exact test was based on the hypergeometric distribution to combine the results of the proportion of the miRNA target gene in the functional gene set and the proportion of miRNA target gene in the whole genome. A P-value for the null hypothesis of the Fisher's exact test was examined as the genes that belong to the target genes of miRNAs and the genes that belong to the functional genes enriched.

The resulting P-value depicts the probability that the examined pathway is significantly enriched with gene targets of the selected miRNAs, the probability that at least  $x$  functional genes are enriched in the  $K$  target genes of miRNA. The P-value can be expressed as:

$$p = 1 - \sum_{i=0}^{x-1} \frac{\binom{M}{i} \binom{N-M}{K-i}}{\binom{N}{K}}$$

Where  $N$  is the total number of genes,  $M$  is the number of genes in the functional genes set and  $K$  is the number of target genes of miRNA.

## Results

**Screening of DEGs and differentially expressed miRNAs.** For GSE15227, 846 and 1,137 DEGs were identified in grade III and IV discs, respectively. For GSE34095, a total of 961 DEGs were identified in the IDD samples compared with the controls. Furthermore, for GSE19943, 77 differentially expressed miRNAs were identified in the degenerative NP samples compared with the controls.

**Grade-specific network construction.** The grade-specific networks are shown in Figs. 1 and 2. In the present study, 746 grade III-specific genes and 964 grade IV-specific genes were identified. Tumor protein p53 (*TP53*) was a hub gene in the grade III-specific network and ubiquitin C (*UBC*) was identified to be a hub gene in the grade IV-specific network. Additionally, there were 78 common genes in these 2 grade-specific networks. Network topology analysis showed that a total of 16 network features were identified. In addition, statistical regression analysis revealed that 6 significant network features were obtained, as shown in Table I, including average shortest path length, betweenness centrality, closeness centrality, neighborhood connectivity, radiality and stress.

**Clustering analysis.** The clustering analysis was used to group the genes and samples on the basis of similarities of gene expression. The results of clustering analysis using all the specific genes in these 2 networks are shown in Fig. 3A. The result showed that 2 grade III samples (GSM380301 and GSM380305) were grouped into the region of grade IV samples; however, the correlation was lower compared to the correlation of the grade IV samples. By contrast, the results of clustering analysis using the top 20% genes with a higher degree in these 2 networks are shown in Fig. 3B. Consistently, the 2 grade III samples, GSM380301 and GSM380305, were grouped into the region of grade IV samples.

Table I. Logistic regression.

Feature	P-value	Exp (B)
Average shortest path length	<0.0001	0.050
Betweenness centrality	<0.0001	<0.0001
Closeness centrality	<0.0001	<0.0001
Neighborhood connectivity	0.030	1.015
Radiality	0.036	<0.0001
Stress	<0.0001	1.010
Constant	0.001	1.08x10 <sup>11</sup>

Exp (B) represents odd ratio in the logistic regression model.

Table II. GO terms of grade III-specific genes.

GO term	P-value
Angiogenesis	0.007
Adult walking behavior	0.007
Retina development in camera-type eye	0.008
Activation of protein kinase activity	0.008
Response to DNA damage stimulus	0.008
Negative regulation of biosynthetic process	0.009
Negative regulation of cellular biosynthetic process	0.011
Negative regulation of macromolecule biosynthetic process	0.014
Positive regulation of protein kinase activity	0.015
Positive regulation of kinase activity	0.020
Cytokine secretion	0.024
Negative regulation of gene expression	0.024
Negative regulation of transcription	0.025
Positive regulation of transferase activity	0.026
Negative regulation of nucleobase, nucleoside, nucleotide and nucleic acid metabolic process	0.029
Negative regulation of nitrogen compound metabolic process	0.034
Vasculature development	0.037
Patterning of blood vessels	0.038
Tube morphogenesis	0.039
Regulation of protein kinase activity	0.043
Adult locomotory behavior	0.044
Actin filament organization	0.044
Cell-substrate junction assembly	0.048
Negative regulation of macromolecule metabolic process	0.050

GO, Gene Ontology.

**GO and pathway enrichment analysis of specific genes.** GO and pathway analysis indicated that grade III- and IV-specific genes were significantly enriched in different GO terms and KEGG pathways. A total of 23 GO terms for grade III-specific genes were enriched, including angiogenesis, adult walking behavior and positive regulation of kinase activity (Table II).

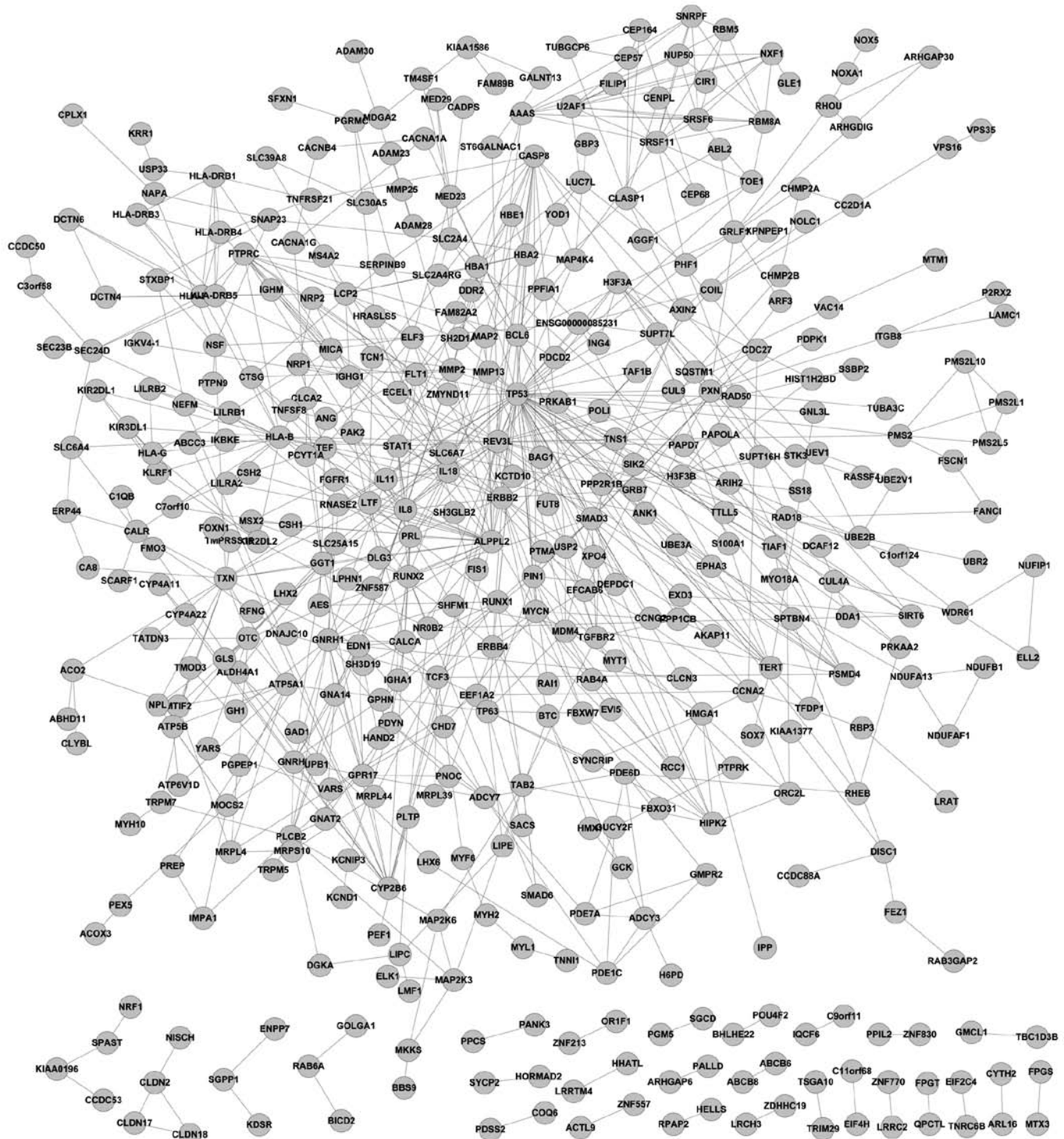


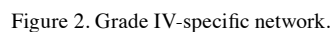
Figure 1. Grade III-specific network.

GO terms for grade IV-specific genes were mainly associated with the regulation of ubiquitin-protein ligase activity, such as positive regulation of ubiquitin-protein ligase activity, and regulation of protein ubiquitination (Table III). In addition, 4 KEGG pathways for grade III-specific genes were significantly enriched, including Alzheimer's disease, oxidative phosphorylation, Huntington's disease and Parkinson's disease. A total of 5 KEGG pathways for grade IV-specific genes were significantly enriched, including viral myocarditis,

graft-versus-host disease, type I diabetes mellitus, allograft rejection and cell adhesion molecules (Table IV).

*miRNA-pathway-genes complex regulatory associations analysis.* Subsequent to combining miRecords, miRTarBase and TarBase 6.0 databases, 5,489 miRNA-target pairs were collected in the study, including 482 miRNAs and 2,331 target genes. miRNA-pathway interactions analysis showed that there were 217 interaction pairs involved in 35 significant





The general concepts, such as centrality, communicability and betweenness, quantify the important features in a network (34). Estrada (35) demonstrated that subgraph centrality could be applied to the identification of essential proteins in PPI networks. Additionally, the threshold for inclusion was  $P < 0.05$  (significant) in the logistic regression model (36). In line with the previous study, the present study showed that 6 network features (average shortest path length, betweenness centrality, closeness centrality, neighborhood connectivity, radiality and stress) had significant differences

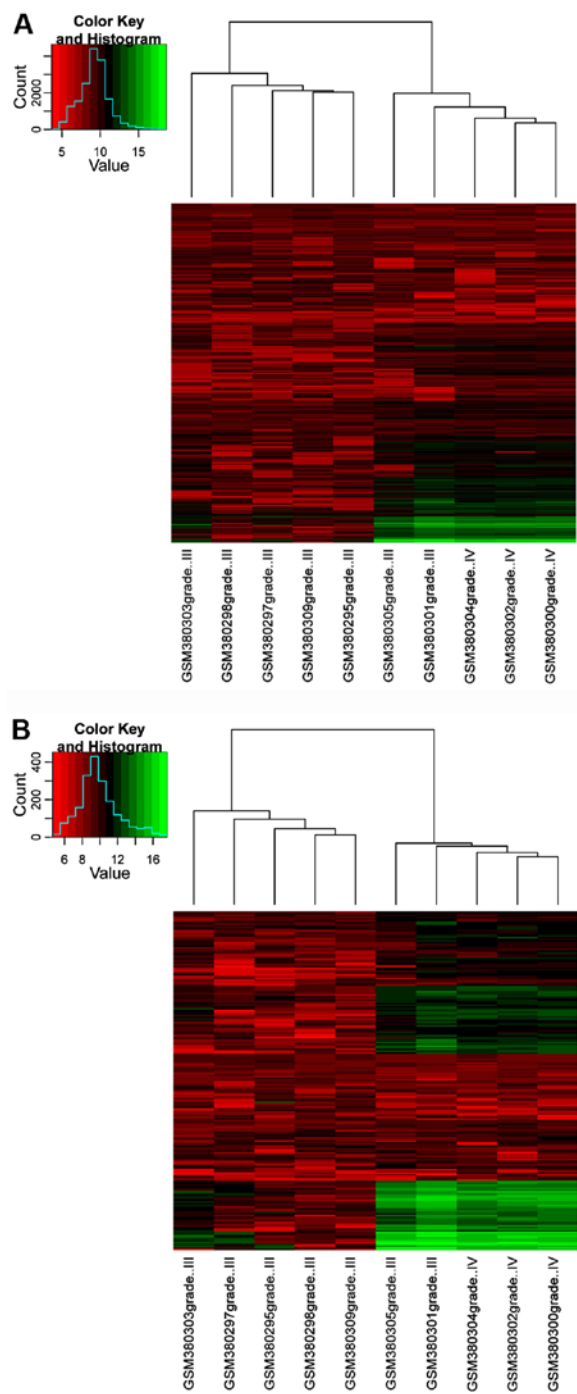


Figure 3. Heat-maps of specific genes. (A) Heat-maps of all the specific genes in 2 grade-specific networks. (B) Heat-maps of the top 20% specific genes that had higher degrees in the grade-specific networks. The red color indicates a high expression level and the green color indicates a low expression level of a specific gene in a particular specimen.

in grade III- and IV-specific networks (Table I). On this basis, these 6 features may have a significant association with the grade of discs degeneration and could be useful for assessing the IDD grade.

TP53 is a tumor-suppressor protein containing DNA binding, transcriptional activation and oligomerization domains (37). Vaghefi *et al* (38) revealed that deacetylation of p53 was a nerve growth factor (NGF)-dependent post-translational mechanism of p53 activation. Additionally,

Table III. GO terms of grade IV-specific genes.

GO terms	P-value
Cellular macromolecule localization	0.036
Cellular protein localization	0.030
Establishment of protein localization	0.026
Intracellular protein transport	0.038
Positive regulation of ligase activity	0.031
Positive regulation of protein ubiquitination	0.039
Positive regulation of ubiquitin-protein ligase activity	0.019
Positive regulation of ubiquitin-protein ligase activity during mitotic cell cycle	0.013
Protein transport	0.036
Regulation of ligase activity	0.025
Regulation of protein ubiquitination	0.022
Regulation of ubiquitin-protein ligase activity	0.015
Regulation of ubiquitin-protein ligase activity during mitotic cell cycle	0.022

GO, Gene Ontology.

Table IV. Pathway enrichment of grade III- and IV-specific genes.

Pathway	P-value
Grade III	
hsa05010: Alzheimer's disease	0.009
hsa00190: Oxidative phosphorylation	0.011
hsa05016: Huntington's disease	0.012
hsa05012: Parkinson's disease	0.021
Grade IV	
hsa05416: Viral myocarditis	9.37x10 <sup>-4</sup>
hsa05332: Graft-versus-host disease	0.012
hsa04940: Type I diabetes mellitus	0.017
hsa05330: Allograft rejection	0.040
hsa04514: Cell adhesion molecules	0.049

Richardson *et al* (39) reported that NGF had increased expression in the painful degenerate intervertebral disc. In addition, Liu *et al* (40) demonstrated that *VEGF* and *p53* were working simultaneously in neovascularization and infiltration, and accelerating rat IDD progression. In line with the previous study, TP53 was identified as a hub gene in the grade III-specific network, which was derived from the microarray data of GSE15227. Furthermore, specimens of GSE15227 are annulus fibrosus cells in cultures from patients with herniated discs and IDD. Thus, we hypothesized that TP53 may participate in neovascularization and infiltration in annulus fibrosus in IDD progression, which could also help the IDD grading system.

Additionally, the present study identified that the GO terms for grade IV-specific genes were mainly associated with the regulation of ubiquitin-protein ligase activity and



*UBC* was a hub gene in the grade IV-specific network derived from the data of GSE15227. *UBC* encodes a poly-ubiquitin precursor that can conjugate with different residues and lead to various effects within a cell (41). Yew (42) demonstrated that G1- and S-phase events in vertebrates, which were essential for cell proliferation, were specifically mediated by a multitude of regulators associated with ubiquitination, of which *UBC* was required. Furthermore, Gruber *et al* (43) reported that cells in IDD lost their ability to proliferate and were subject to senescence. Thus, we hypothesized that *UBC* may have a crucial role in inhibiting cell proliferation of annulus fibrosus in IDD progression and could be used for grading disc degeneration.

Furthermore, the present study showed that miR-129-5p could participate in different pathways, including apoptosis. The study by Kohyama *et al* (44) reported that induction of the apoptosis of disc cells had an important role in the pathogenesis of disc degeneration. In addition, Li *et al* (45) revealed that downregulation of miR-129-5p could inhibit cell growth and induce apoptosis in laryngeal squamous cell carcinoma by targeting adenomatous polyposis coli. In the present study, the miRNA-pathway interaction analysis was based on the information of differentially expressed miRNAs derived from GSE19943 and the pathway enrichment analysis for DEGs in degenerative NP samples was derived from GSE34095. Additionally, tissues of GSE19943 and GSE34095 are NP from patients with IDD and scoliosis. Furthermore, 6 overlapping pathways were identified according to the results of miRNA-pathway interactions analysis and pathway enrichment analysis for DEGs, including apoptosis. Therefore, we hypothesized that miR-129-5p may have a crucial role in modulating cell apoptosis in NP in IDD progression and miR-129-5p could be a potential therapeutic target for IDD. However, more experiments and further investigations are required to verify this finding.

In conclusion, the present study identified that key genes (*TP53* and *UBC*) and miR-129-5p may participate in the mechanism of IDD progression. Significant network features identified in the study may aid in assessing the grade of disc degeneration. *TP53* may have an essential role in neovascularization and infiltration in annulus fibrosus in grade III of IDD progression and could help the IDD grading system. Additionally, *UBC* may have a crucial role in inhibiting cell proliferation of annulus fibrosus in IDD progression and could be used to grade disc degeneration. Furthermore, miR-129-5p may have a crucial role in modulating cell apoptosis in NP in IDD progression and miR-129-5p could be a potential therapeutic target for IDD. However, further experiments and studies are required to confirm these results.

## Acknowledgements

The present study was supported by the National Natural Science Foundation of China: The effect and mechanism of cytoskeletal elements in the mechanotransduction pathway within intervertebral disc cells and its role in intervertebral disc degeneration (grant no. 81471131) and the National Natural Science Foundation of China: The effect and mechanism of chondroitin sulphate proteoglycans in stem cell niche during stem cell differentiation (grant no. 31300675).

## References

1. Hadjipavlou AG, Tzermiadianos MN, Bogduk N and Zindrick MR: The pathophysiology of disc degeneration: A critical review. *J Bone Joint Surg Br* 90: 1261-1270, 2008.
2. Wang SZ, Rui YF, Tan Q and Wang C: Enhancing intervertebral disc repair and regeneration through biology: Platelet-rich plasma as an alternative strategy. *Arthritis Res Ther* 15: 220, 2013.
3. Yoritoku E, Chiba K, Toyama Y and Hirabayashi K: Long-term outcomes of standard discectomy for lumbar disc herniation: A follow-up study of more than 10 years. *Spine* 26: 652-657, 2001.
4. Karasek M and Bogduk N: Twelve-month follow-up of a controlled trial of intradiscal thermal anuloplasty for back pain due to internal disc disruption. *Spine* 25: 2601-2607, 2000.
5. Anderson PA and Rouleau JP: Intervertebral disc arthroplasty. *Spine* 29: 2779-2786, 2004.
6. Shimer AL, Chadderdon RC, Gilbertson LG and Kang JD: Gene therapy approaches for intervertebral disc degeneration. *Spine* 29: 2770-2778, 2004.
7. Choi YS: Pathophysiology of degenerative disc disease. *Asian Spine J* 3: 39-44, 2009.
8. Tang Y, Wang S, Liu Y and Wang X: Microarray analysis of genes and gene functions in disc degeneration. *Exp Ther Med* 7: 343-348, 2014.
9. Antoniou J, Epure LM, Michalek AJ, Grant MP, Iatridis JC and Mwale F: Analysis of quantitative magnetic resonance imaging and biomechanical parameters on human discs with different grades of degeneration. *J Magn Reson Imaging* 38: 1402-1414, 2013.
10. Thompson JP, Pearce RH, Schechter MT, Adams ME, Tsang IK and Bishop PB: Preliminary evaluation of a scheme for grading the gross morphology of the human intervertebral disc. *Spine* 15: 411-415, 1990.
11. Pfirrmann CW, Metzendorf A, Zanetti M, Hodler J and Boos N: Magnetic resonance classification of lumbar intervertebral disc degeneration. *Spine* 26: 1873-1878, 2001.
12. Adams MA and Roughley PJ: What is intervertebral disc degeneration, and what causes it? *Spine* 31: 2151-2161, 2006.
13. Bachmeier BE, Nerlich A, Mittermaier N, Weiler C, Lumenta C, Wuerz K and Boos N: Matrix metalloproteinase expression levels suggest distinct enzyme roles during lumbar disc herniation and degeneration. *Eur Spine J* 18: 1573-1586, 2009.
14. Takahashi M, Haro H, Wakabayashi Y, Kawa-uchi T, Komori H and Shinomiya K: The association of degeneration of the intervertebral disc with 5a/6a polymorphism in the promoter of the human matrix metalloproteinase-3 gene. *J Bone Joint Surg Br* 83: 491-495, 2001.
15. Pratsinis H and Kleissas D: PDGF, bFGF and IGF-I stimulate the proliferation of intervertebral disc cells in vitro via the activation of the ERK and Akt signaling pathways. *Eur Spine J* 16: 1858-1866, 2007.
16. van Rooij E and Kauppinen S: Development of microRNA therapeutics is coming of age. *EMBO Mol Med* 6: 851-864, 2014.
17. Yu X, Li Z, Shen J, Wu WK, Liang J, Weng X and Qiu G: MicroRNA-10b promotes nucleus pulposus cell proliferation through RhoC-Akt pathway by targeting HOXD10 in intervertebral disc degeneration. *PLoS One* 8: e83080, 2013.
18. Chen Y, Chen K, Li M, Li C, Ma H, Bai YS, Zhu XD and Fu Q: Genes associated with disc degeneration identified using microarray gene expression profiling and bioinformatics analysis. *Genet Mol Res* 12: 1431-1439, 2013.
19. Wang HQ, Yu XD, Liu ZH, Cheng X, Samartzis D, Jia LT, Wu SX, Huang J, Chen J and Luo ZJ: Deregulated miR-155 promotes Fas-mediated apoptosis in human intervertebral disc degeneration by targeting FADD and caspase-3. *J Pathol* 225: 232-242, 2011.
20. Gruber HE, Hoelscher G, Loeffler B, Chow Y, Ingram JA, Halligan W and Hanley EN Jr: Prostaglandin E1 and misoprostol increase epidermal growth factor production in 3D-cultured human annulus cells. *Spine* J 9: 760-766, 2009.
21. Tsai TT, Lai PL, Liao JC, Fu TS, Niu CC, Chen LH, Lee MS, Chen WJ, Fang HC, Ho NY, *et al*: Increased periostin gene expression in degenerative intervertebral disc cells. *Spine* J 13: 289-298, 2013.
22. Gentleman R, Carey VJ, Huber W, Irizarry RA and Dudoit S (eds): Bioinformatics and computational biology solutions using R and Bioconductor. Springer, 2005.
23. Benjamini Y and Hochberg Y: Controlling the false discovery rate: A practical and powerful approach to multiple testing. *J R Stat Soc B* 57: 289-300, 1995.

24. Xiao F, Zuo Z, Cai G, Kang S, Gao X and Li T: miRecords: An integrated resource for microRNA-target interactions. *Nucleic Acids Res* 37: D105-D110, 2009.
25. Hsu SD, Lin FM, Wu WY, Liang C, Huang WC, Chan WL, Tsai WT, Chen GZ, Lee CJ, Chiu CM, *et al*: miRTarBase: A database curates experimentally validated microRNA-target interactions. *Nucleic Acids Res* 39: D163-D169, 2011.
26. Vergoulis T, Vlachos IS, Alexiou P, Georgakilas G, Maragkakis M, Reczko M, Gerangelos S, Koziris N, Dalamagas T and Hatzigeorgiou AG: TarBase 6.0: Capturing the exponential growth of miRNA targets with experimental support. *Nucleic Acids Res* 40: D222-D229, 2012.
27. Kanehisa M and Goto S: KEGG: Kyoto encyclopedia of genes and genomes. *Nucleic Acids Res* 28: 27-30, 2000.
28. Smoot ME, Ono K, Ruscheinski J, Wang PL and Ideker T: Cytoscape 2.8: New features for data integration and network visualization. *Bioinformatics* 27: 431-432, 2011.
29. Franceschini A, Szklarczyk D, Frankild S, Kuhn M, Simonovic M, Roth A, Lin J, Minguez P, Bork P, von Mering C, *et al*: STRING v9.1: Protein-protein interaction networks, with increased coverage and integration. *Nucleic Acids Res* 41: D808-D815, 2013.
30. Assenov Y, Ramírez F, Schelhorn S-E, Lengauer T and Albrecht M: Computing topological parameters of biological networks. *Bioinformatics* 24: 282-284, 2008.
31. Huang Y, Pepe MS and Feng Z: Logistic regression analysis with standardized markers. *Ann Appl Stat* 7: 7, 2013.
32. Sherman BT, Huang da W, Tan Q, Guo Y, Bour S, Liu D, Stephens R, Baseler MW, Lane HC and Lempicki RA: DAVID Knowledgebase: A gene-centered database integrating heterogeneous gene annotation resources to facilitate high-throughput gene functional analysis. *BMC Bioinformatics* 8: 426, 2007.
33. Blevins L and McDonald C: Fisher's Exact Test: an easy-to-use statistical test for comparing outcomes. *MD Comput* 2: 15, 1985.
34. Estrada E and Higham DJ: Network properties revealed through matrix functions. *SIAM Rev* 52: 696-714, 2010.
35. Estrada E: Virtual identification of essential proteins within the protein interaction network of yeast. *Proteomics* 6: 35-40, 2006.
36. Tailor A, Jurkovic D, Bourne TH, Collins WP and Campbell S: Sonographic prediction of malignancy in adnexal masses using multivariate logistic regression analysis. *Ultrasound Obstet Gynecol* 10: 41-47, 1997.
37. Dumont P, Leu JI, Della Pietra AC III, George DL and Murphy M: The codon 72 polymorphic variants of p53 have markedly different apoptotic potential. *Nat Genet* 33: 357-365, 2003.
38. Vaghefi H and Neet KE: Deacetylation of p53 after nerve growth factor treatment in PC12 cells as a post-translational modification mechanism of neurotrophin-induced tumor suppressor activation. *Oncogene* 23: 8078-8087, 2004.
39. Richardson SM, Doyle P, Minogue BM, Gnanalingham K and Hoyland JA: Increased expression of matrix metalloproteinase-10, nerve growth factor and substance P in the painful degenerate intervertebral disc. *Arthritis Res Ther* 11: R126, 2009.
40. Liu XW, Kang J, Fan XD and Sun LF: Expression and significance of VEGF and p53 in rat degenerated intervertebral disc tissues. *Asian Pac J Trop Med* 6: 404-406, 2013.
41. Marinovic AC, Zheng B, Mitch WE and Price SR: Ubiquitin (UbC) expression in muscle cells is increased by glucocorticoids through a mechanism involving Sp1 and MEK1. *J Biol Chem* 277: 16673-16681, 2002.
42. Yew PR: Ubiquitin-mediated proteolysis of vertebrate G1- and S-phase regulators. *J Cell Physiol* 187: 1-10, 2001.
43. Gruber HE, Ingram JA, Norton HJ and Hanley EN Jr: Senescence in cells of the aging and degenerating intervertebral disc: Immunolocalization of senescence-associated  $\beta$ -galactosidase in human and sand rat discs. *Spine* 32: 321-327, 2007.
44. Kohyama K, Saura R, Doita M and Mizuno K: Intervertebral disc cell apoptosis by nitric oxide: Biological understanding of intervertebral disc degeneration. *Kobe J Med Sci* 46: 283-295, 2000.
45. Li M, Tian L, Wang L, Yao H, Zhang J, Lu J, Sun Y, Gao X, Xiao H and Liu M: Down-regulation of miR-129-5p inhibits growth and induces apoptosis in laryngeal squamous cell carcinoma by targeting APC. *PLoS One* 8: e77829, 2013.